Source Wave Distortion Resulting From Total Internal Reflections

As outlined in Technical Note 7, entitled "Reflection Coefficient Estimation for DST Blind Seismic Deconvolution Test Bed Simulation", angles of incidents that exceed the critical angle result in Total Internal Reflections (TIRs). TIRs are commonly incurred during downhole and crosshole seismic testing and result in source wave distortions due to the fact that the reflection coefficients become complex.

As mentioned in Technical Note 7 the SH *precritical reflection coefficient* (reflections at angles less than the critical angle) is:

$$R = \frac{A_1}{A_0} = \frac{G_1\eta_1 - G_2\eta_2}{G_1\eta_1 + G_2\eta_2} = \frac{\rho_1 V_1 cos\theta_1 - \rho_2 V_2 cos\theta_2}{\rho_1 V_1 cos\theta_1 + \rho_2 V_2 cos\theta_2} \tag{1}$$

The SH *post-critical reflection coefficient can then be* given as

$$R = \frac{A_1}{A_0} = \frac{G_1\acute{\eta}_1 - iG_2\acute{\eta}_2}{G_1\acute{\eta}_1 + iG_2\acute{\eta}_2} = \frac{e^{-i\alpha}}{e^{+i\alpha}} = e^{-i2\alpha} \tag{2}$$

with

$$\alpha = tan^{-1}\left(\frac{G_2\acute{\eta}_2}{G_1\acute{\eta}_1}\right) \tag{3}$$

where R is the reflection coefficient, A_0 is the amplitude of incident, A_1 is the amplitude of reflected wave, $G_1$and G_2 denote the shear modulus of mediums 1 and 2, respectively, i is the imaginary number, and $\acute{\eta}_1$ and $\acute{\eta}_2$ denote the *post-critical* vertical slowness within mediums 1 and 2, respectively, which can be given as:

$$\acute{\eta}_1 = \sqrt{u_1^2 - p^2} \tag{4a}$$

$$\acute{\eta}_2 = \sqrt{p^2 - u_2^2} \tag{4b}$$

where p is the ray parameter.

The seismogram for TIRs is generated by convolving the source waves by the reflection coefficients given in eq. (2) for various incident angles that exceed the critical angle. In the frequency domain this is equivalent to multiplying the source wave by the reflection coefficients given by eq. (2) producing a frequency-independent phase shift as shown below:

$$\begin{aligned} U &= RA_0 e^{i(kx-\omega t)} \\ &= A_0 e^{-i2\alpha} e^{i(kx-\omega t)} \\ &= A_0 e^{i\left(kx-\omega(t+2\alpha/\omega)\right)} \end{aligned} \tag{5}$$

where parameter k denotes the wave number, x the distance, ω the angular frequency and t the time.

As is evident from eq. (5), the reflected wave has a phase shift of $2\alpha/\omega$ or $2\alpha/2\pi f_d$ where f_d is the dominant frequency of the source wave.

It can be shown (Aki and Richards, 2002, pg 153) that any phase shift of a source wave can be determined from the source wave and its Hilbert transform as follows

$$\hat{f}(t) = \cos\alpha\, f(t) + sin\alpha \mathrm{H}[f(t)] \tag{6}$$

where $\hat{f}(t)$ is the phase shifted source wave, *f(t)* is the original source wave, α is the phase shift and *H[f(t)]* is the Hilbert transform of the source wave, which introduces a 90° phase shift of a function (i.e., $R = -i$ in eq. (2)).

Two commonly utilized analytical source waves in seismic signal processing are the Berlage source wave and the Ricker source wave. To provide illustrative examples of the phase shifting of seismic source waves due to TIRs eq. (6) was applied on both these source waves.

In Figures 1 to 5 below, the red time series is a Berlage source wave with a dominant frequency of 55 Hz. The green time series in Figures 1 to 5 are the inputted Berlage source wave phase shifted by 40°, 60°, 90°, 120° and 220°, respectively.

In Figures 6 to 10, the red time series is a Ricker source wave with a dominant frequency of 50 Hz. The green time series in Figures 6 to 10 are the inputted Ricker source wave phase shifted by 40°, 60°, 90°, 120° and 220°, respectively.

As is demonstrated in these figures for both the Berlage and Ricker source waves, even though the dominant frequency has been retained, the source waves have been phase shifted within the envelope of the wave packet and the minimum and maximum peaks have been modified (i.e., note that the 2 waves have the same arrival time (causal) but different phases and minima and maxima) resulting in source wave distortion.

This impact of the phase shift introduce a significant seismic signal processing challenge in DST and in crosshole seismic testing and therefore the presence of TIRs requires that a blind seismic deconvolution technique that allows for time variant source waves is utilized for data processing.

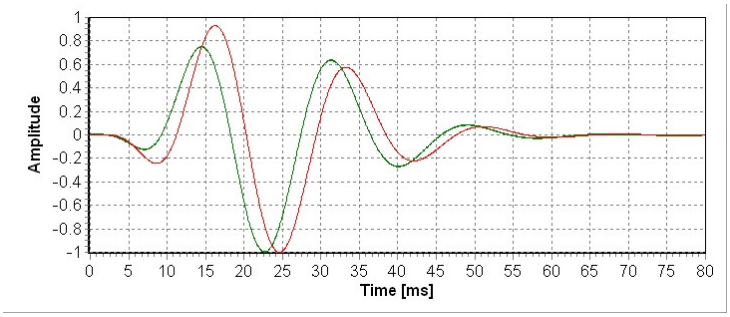

Figure 1. Berlage source wave - 40° phase shift.

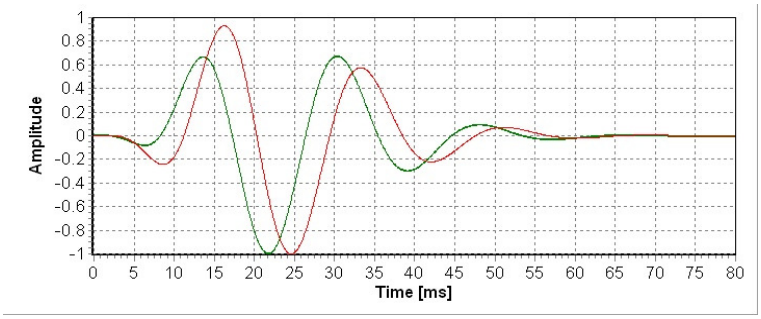

Figure 2. Berlage source wave - 60° phase shift.

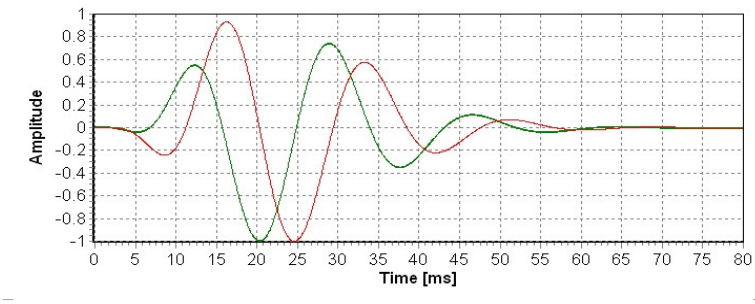

Figure 3. Berlage source wave - 90° phase shift.

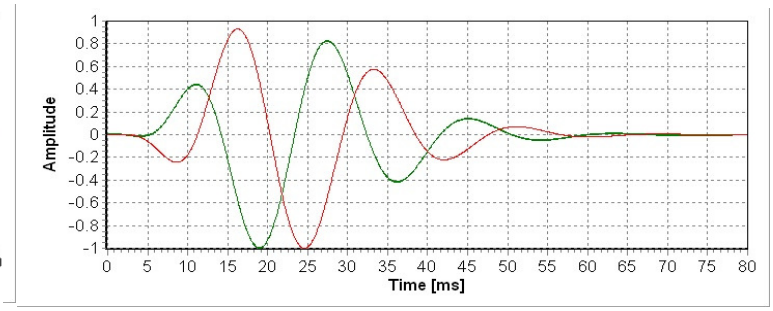

Figure 4. Berlage source wave - 120° phase shift.

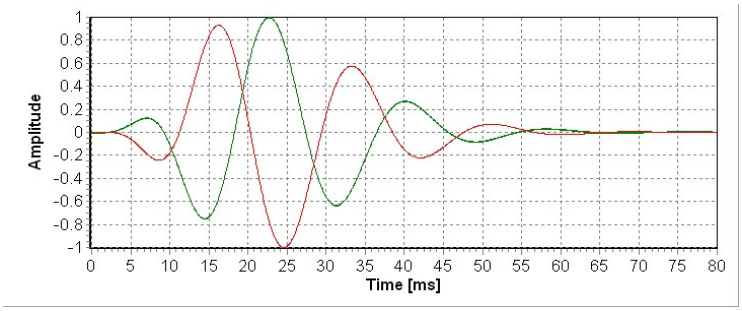

Figure 5. Berlage source wave - 220° phase shift.

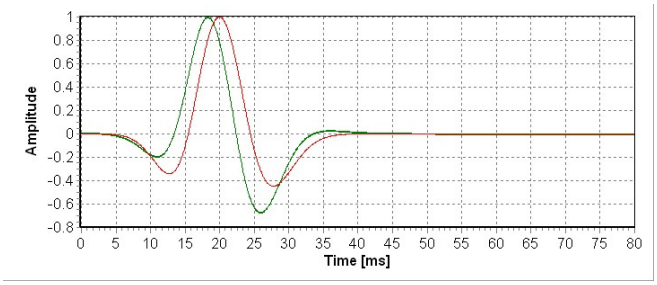

Figure 6. Ricker source wave - 40° phase shift.

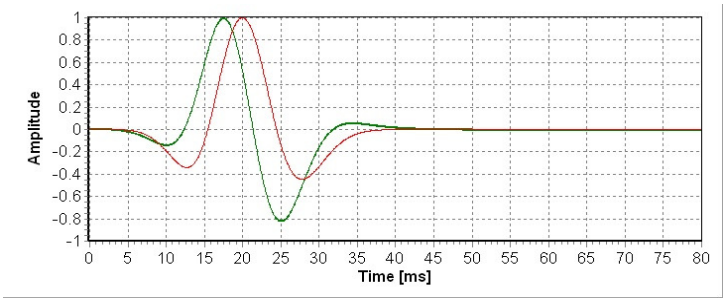

Figure 7. Ricker source wave - 60° phase shift.

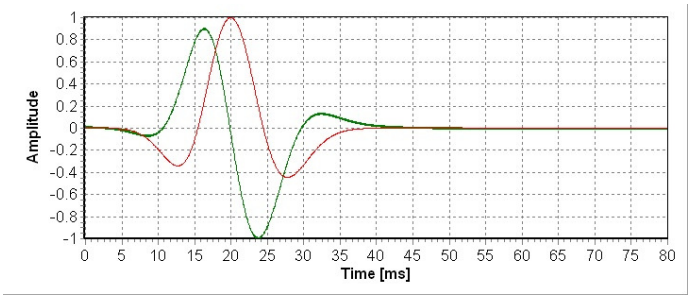

Figure 8. Ricker source wave - 90° phase shift.

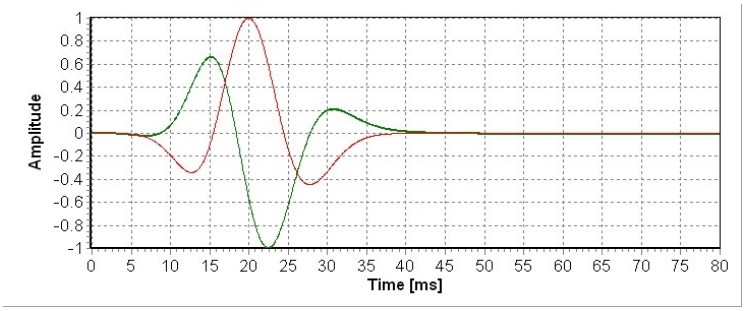

Figure 9. Ricker source wave - 120° phase shift.

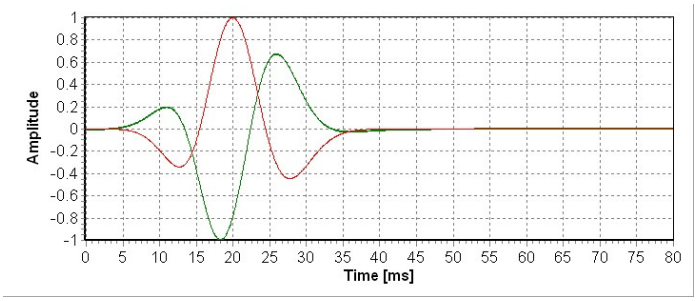

Figure 10. Ricker source wave - 220° phase shift.

Erick Baziw
Gerald Verbeek

BCE's mission is to provide our clients around the world with state-of-the-art seismic data acquisition and analysis systems, which allow for better and faster diagnostics of the sub-surface. Please visit our website (www.bcengineers.com) or contact our offices for additional information:

e-mail: info@bcengineers.com

phone: Canada: (604) 733 4995 – USA: (903) 216 5372